



Electrical Capacitance to High-resolution Observation (ECHO)
2025 Human Lander Challenge Technical Paper
Embry-Riddle Aeronautical University

Bruce Noble
Undergraduate
Project Manager
Aerospace Engineering
nobleb2@my.erau.edu

Grant Bowers
Undergraduate
Deputy Project Manager
Software Engineering
bowersg3@my.erau.edu

David Clay
Undergraduate
Media Officer
Aerospace Engineering
clayd6@my.erau.edu

Jakobe Denby
Undergraduate
Safety Officer
Aerospace Engineering
denbyj@my.erau.edu

Aidan Kihm
Undergraduate
Business Officer
Mechanical Engineering
kihma1@my.erau.edu

Sanaya Nichani
Undergraduate
Testing Officer
Aerospace Engineering
nichans1@my.erau.edu

Max Klein
Undergraduate Researcher
Aerospace Engineering
kleinm8@my.erau.edu

Christopher LeClair
Undergraduate Researcher
Aerospace Engineering
leclair1@my.erau.edu

Ian Naegeli
Undergraduate Researcher
Mechanical Engineering
naegeli@my.erau.edu

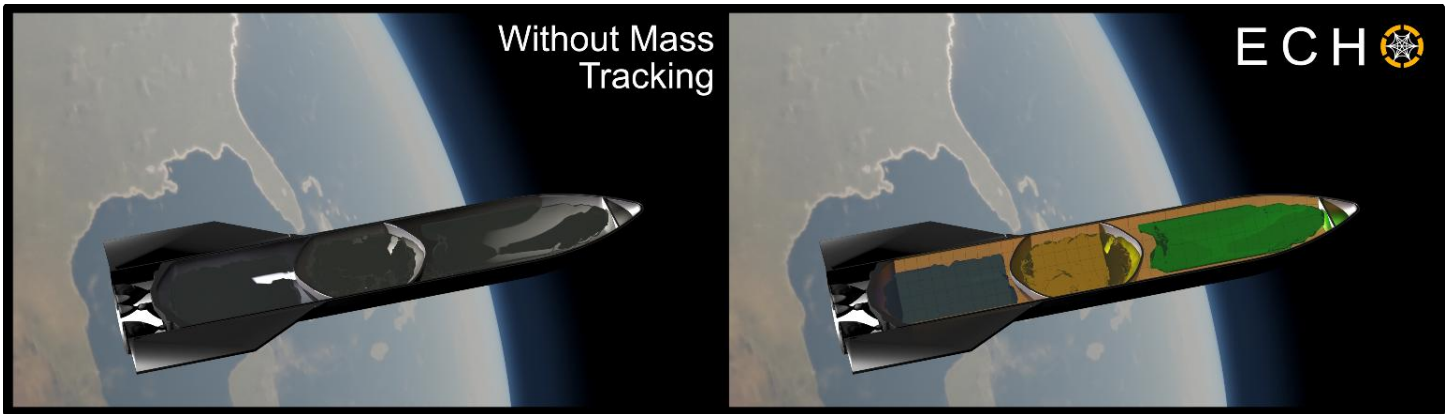
Cooper Nelson
Undergraduate Researcher
Aerospace Engineering
nelsonc7@my.erau.edu

Connor Shackelford
Undergraduate Researcher
Aerospace Engineering
shackec2@my.erau.edu

Owen Smith
Undergraduate Researcher
Mechanical Engineering
smitho10@my.erau.edu

Dr. Siwei Fan
Academic Mentor
Aerospace Engineering
siwei.fan@erau.edu

Dr. Ron Madler
Academic Mentor
Aerospace Engineering
ron.madler@erau.edu



To the HuLC Project Lead: I, Siwei Fan, hereby attest that I have reviewed and approved the proposal submission for the project, titled,

Electrical Capacitance to High-resolution Observation, from Embry-Riddle Aeronautical University, Prescott, AZ (project title) (university)

By signing below, I verify that the submitting team has fulfilled the requirements for my review of the final proposal for the Human Lander Challenge (HuLC) competition. I understand that the electronic signature appearing on this document is the same as a handwritten signature for the purposes of validity and admissibility.

[Handwritten signature of Siwei Fan]
(signature)

May-28-2025
(date)

Table of Contents

Quad Chart.....	5
Technical Paper.....	6
1.1. Executive Summary.....	6
1.2. Problem Statement.....	6
1.3. Solution.....	6
1.4. Changes from Proposal.....	6
1.5. Innovation.....	7
1.5.1. Machine Learning Architecture	7
1.5.2. Machine Learning Overview.....	8
1.5.3. Analysis.....	9
1.6. Future Advancements	10
1.6.1. Electrode Integration.....	10
1.6.2. Domed Geometries.....	10
1.6.3. Relevant Environment Testing.....	11
1.7. Verification.....	11
1.8. Validation	11
1.9. Risks	13
1.10. Full-Scale Implementation	14
1.11. Budget.....	14
1.12. Project Timeline	16
1.13. Conclusion.....	17
References.....	18
Appendix.....	20

Table of Tables

Table 1: ECHO Risks Matrix13

Table 2: PCEC Cost Outputs (Millions of Dollars).....14

Table 3: Full Budget Breakdown (Thousands of Dollars)15

Table 4: Microgravity Mass-Gauging Methods Trade Study20

Table 5: Testing Fluids Trade Study20

Table 6: Machine Learning Algorithms Trade Study20

Table 7: ECHO Risks Matrix21

Table of Figures

Figure 1: Quad Chart5

Figure 2: ECHO Algorithm Training Flowchart8

Figure 3: ECHO Two-Circle Demonstration8

Figure 4: ECHO Four-Circle Demonstration9

Figure 5: ANSYS Maxwell Simulation Setup10

Figure 6: Test Apparatus Section View (Left) and Complete Setup (Right)12

Figure 7: Cross-Section Inserts.....12

Figure 8: Idealized Circle Reconstruction13

Figure 9: ECHO Development Timeline16

Figure 10: Extra Test 123

Figure 11: Extra Test 223

Figure 12: Extra Test 323

Figure 13: Extra Test 424

Figure 14: Extra Test 524

Figure 15: Extra Test 624

Figure 16: Extra Test 725

Figure 17: HLS Starship Progression25

Table of Acronyms

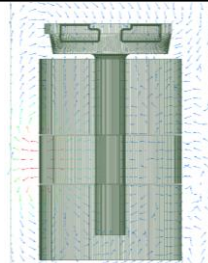
AECVT	Adaptive Electrical Capacitance Volume Tomography
CGAN	Conditional Generative Adversarial Network
CER	Cost Estimating Relationship
DAQ	Data Acquisition
ECHO	Electrical Capacitance to High-resolution Observation
ECT	Electrical Capacitance Tomography
ECVT	Electrical Capacitance Volume Tomography
FEA	Finite Element Analysis
FPC	First Pound Cost
FPCB	Flexible Printed Circuit Board
FY	Fiscal Year
HLS	Human Landing System
HuLC	Human Lander Challenge
IC	Image Correlation
LBP	Linear Back Projection
LN2	Liquid Nitrogen
ME	Mean Error
ML	Machine Learning
NASA	National Aeronautics and Space Administration
PARSEC	Professional Association of Research for Space Engineering Concepts
PCEC	Project Cost Estimating Capability
SM	Sensitivity Matrix
TRL	Technology Readiness Level
\$K	Thousands of Dollars
\$M	Millions of Dollars

Objective

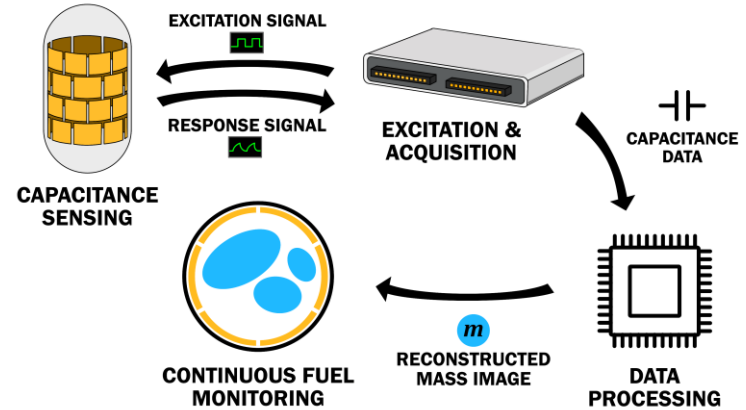
Develop a system that can measure propellant mass and distribution in microgravity.

Technical Approach

- Conduct simulations of a custom Electrical Capacitance Tomography (ECT) electrode array in ANSYS® Maxwell® to obtain electric field datasets.
- Identify and implement a machine learning algorithm to train for ECT image reconstruction
- Design and build a test apparatus with the custom array to validate proposed machine learning algorithm.



Test Apparatus Electric Field Simulation



Sensor Design

- Electrode array lining the interior tank walls
- Electrodes are sequentially excited and inter-electrode capacitance is measured



Starship ECT Concept

Test Apparatus

- Dewar lined by FPCB with single layer of electrodes
- Different cross-sections can be suspended in open air and liquid nitrogen for testing



Test Apparatus Section View

Machine Learning

Algorithm to determine propellant quantity from capacitance measurement data

Convolutional Layers:

Extract features from a matrix of input data with dot products.

Activation Layers:

Add nonlinearity to the network with element-wise operations.

Pooling Layers:

Reduce memory and time taken while limiting overfitting.

Dense Layers:

Perform weighted sum of inputs and applies activation layers.

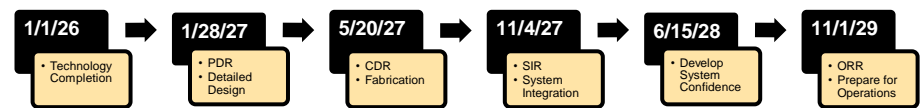


Capacitance Matrix



ML Output Image

Schedule



Cost Estimate for Full-Scale Implementation

Personnel: \$4.4M
 Direct Costs: \$65.5M
 Margin: \$20.9M
 Flight Unit: \$5.5M

Total Non-Recurring: \$90.8M
Total Recurring: \$5.5M



Starship Implementation Concept Image

Figure 1: Quad Chart

Technical Paper

1.1. Executive Summary

As NASA prepares to embark on extended missions to the Moon and Mars, the development of accurate microgravity propellant gauging techniques will be imperative to mission success (Zimmerli, 2007). Current mass gauging techniques are unable to reliably track the quantity of remaining cryogenic propellant or the rate of boil-off with high accuracy during long duration missions. This necessitates that extra propellant is brought to account for the uncertainties. The Professional Association of Research for Space Engineering Concepts (PARSEC) proposes Electrical Capacitance to High-resolution Observation (ECHO) which adapts Electrical Capacitance Tomography (ECT) to work with a machine learning (ML) algorithm to accurately and continuously measure propellant quantities. When implemented, ECHO lines the interior of spacecraft propellant tanks with capacitance measuring electrodes. After making capacitance measurements between electrode pairs, the ML algorithm can rapidly generate and analyze the cross-sectional content of the propellant inside the tank to develop accurate propellant configuration renders.

1.2. Problem Statement

There are two main challenges to cryogenic propellant mass gauging in microgravity: propellant sloshing and boil-off. Sloshing occurs during coasting phases without acceleration, where the propellant is unable to settle and holds no consistent form or location (Lee et al., 2018). The propellant's unpredictable movement requires a mass gauging system that measures the entire tank to acquire accurate readings. Over time, the cryogenic propellant also experiences boil-off, in which the propellant returns to a gaseous state and must be vented due to increasing tank pressure. This process occurs over time, and it is critical to track the lost propellant for mission planning. Current microgravity mass gauging techniques often rely on bookkeeping, calculations using pressure readings, or settled measurements using intermittent acceleration burns (Yendler et al., 2014). Modern mass gauges are also often unable to gauge propellant levels with high accuracy and can be ineffective for different tank configurations (Doherty et al., 2010; Storey et al., 2023). Future propellant mass gauges require a way to continuously determine the propellant quantity, especially for long duration missions.

1.3. Solution

The PARSEC team proposes Electrical Capacitance to High-resolution Observation (ECHO), a solution capable of continuously gauging propellant quantities in microgravity conditions. ECHO aligns with the "Microgravity Mass Tracking of Cryogenics" category in the *2025 Proposal Guidelines for the Human Lander Challenge* and integrates ECT technology with an ML algorithm (HuLC, 2024). To generate cross-sectional images of propellant distribution and determine propellant mass, ECHO utilizes an electrode array that lines the interior of the tank and takes continuous capacitance measurements of the tank's contents. The ML algorithm then uses capacitance measurements to reconstruct a 2D cross-sectional representation of the internal propellant and determines the propellant configuration. After interpolating between stacked cross-sections throughout the tank, a propellant mass estimate can be inferred.

1.4. Changes from Proposal

Since the initial proposal, the PARSEC team has determined the use of Linear Back Projection (LBP) to be redundant and has made several changes to the testing setup (Wanta et al., 2024). Specifically, since the ML algorithm is capable of reconstructing cross-sectional images using raw capacitance data, the LBP algorithm has been removed from the solution. Through a trade study (Table 5), PARSEC decided to prioritize testing efficiency and proceeded to test the system with air rather than oil. Subsequently, time constraints prevented the use of cryogenic liquids during testing. Despite this limitation, simulations were conducted to continue developing the algorithm. Additionally, the timeline and cost matrix have been

modified to account for a longer development process due to the project's low TRL, including more accurate material cost estimates.

1.5. Innovation

Traditional approaches to ECT reconstruction involve using algorithms such as LBP or the Landweber Iteration to solve ECT's ill-posed inverse problem. The soft-field nature of ECT comes from the limited amount of data each electrode scan can provide, which leads to low-resolution or inaccurate reconstructions (York, 2001). Algorithms like LBP and Landweber do well to mitigate the issues caused by this problem. However, these algorithms are still too inaccurate, slow, or resource intensive to be widely adopted in space applications (Sun et al., 2021; Zheng et al., 2018). ECHO aims to replace the need for these algorithms by using an ML model to rapidly interpret relationships between the measurement data and the real cross-section in the tank for fast and accurate cross-sectional reconstructions.

1.5.1. Machine Learning Architecture

The ECHO algorithm takes an input of a capacitance measurement received from scanning electrodes, and outputs a reconstructed image. ECHO's algorithm is based on a Conditional Generative Adversarial Network (CGAN), which is typically comprised of two smaller ML components, a "generator" and a "discriminator" (Mirza & Osindero, 2014). ECHO's architecture was aimed at CGANs due to the results of a trade study conducted (Table 6). During the model's training, a "real cross-section" is generated, which serves as a ground truth for training. This cross-section undergoes an electrode scanning simulation, which is intended to mimic the electrode scans of a physical system. A 15-electrode setup, like the one the current model of the ECHO system is based on, will generate 105 unique measurements after skipping electrode pairs that have already been scanned. It should be noted that this scanning algorithm is not completely accurate to an ECT scan, although it is meant to mimic one. Information from this scan is passed to a diagonalization algorithm, which rotates the 105 values in a counterclockwise fashion, resulting in a diagonalized square capacitance matrix with a size of 105x105 pixels. This rotation invariance technique is utilized to ensure that the ML algorithm functions, even if the scanning pattern is altered to start with a different electrode than initially trained with (Deabes & Abdel-Hakim, 2024). The generator in ECHO's architecture receives the capacitance matrix and attempts to reconstruct a cross-section that resembles the original image. The reconstructed cross-section and original cross-section are then passed to the discriminator, which is responsible for assigning a real or reconstruction probability value to each image. This confidence value is based on which image the discriminator believes is the real image, and which is the reconstructed image. After these values are assigned, they are passed back to the generator. As the generator is incentivized to make the most realistic images possible, these scores help guide the algorithm. This is visually displayed in Figure 2, which shows the flow of data within the algorithm's training cycle.

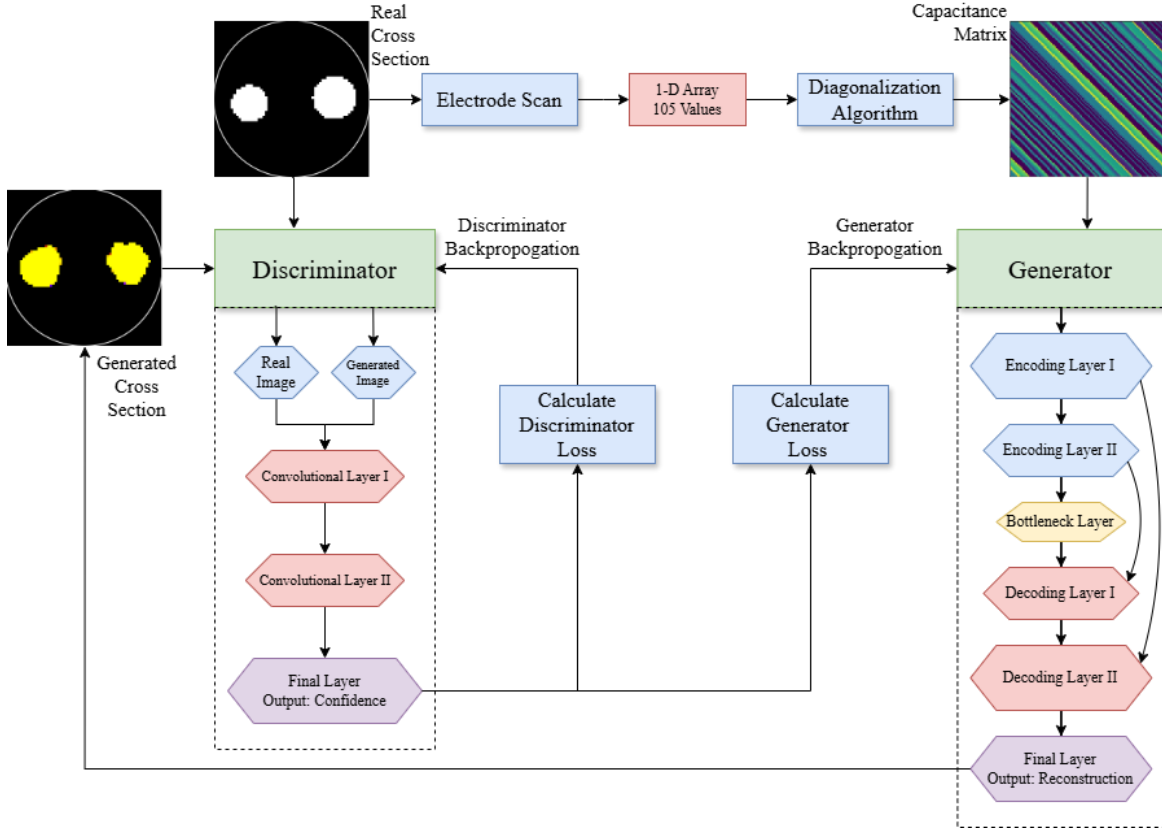


Figure 2: ECHO Algorithm Training Flowchart

1.5.2. Machine Learning Overview

Figure 3 displays the four main steps that the ECHO algorithm takes to gather cross-sectional data: user input, ground truth of the input, capacitance matrix, and image reconstruction. The leftmost plot contains a dynamic input of objects in the sensing area, and in the current simulation, two circles are present. In a spacecraft, this may represent two spheres of floating fuel, bisected into a two-dimensional plane. The “Input” image is then down-sampled into a 64x64 quality map, labeled “Ground Truth.” Then, a scanning algorithm simulates the electrode scanning pattern across the sensing area, which begins to build the capacitance data plot.

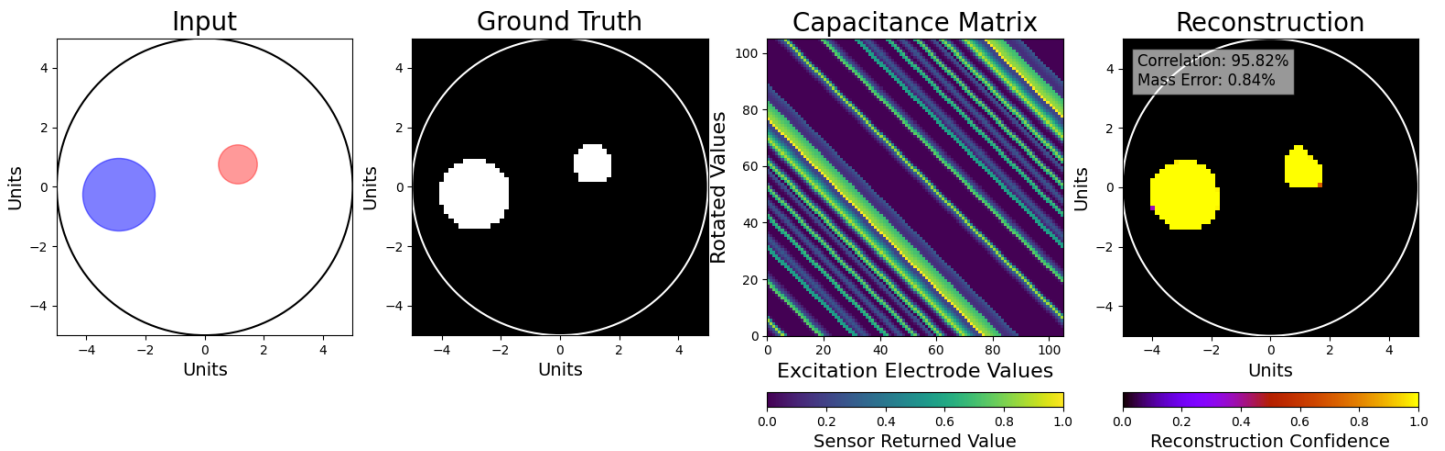


Figure 3: ECHO Two-Circle Demonstration

This specific simulation uses a 15-electrode configuration to build the capacitance matrix, which contains 105 unique values. The diagonalized capacitance matrix is fed through the ECHO algorithm, which returns the attempted reconstruction labeled “Reconstruction.” In this case, the ECHO algorithm’s attempt to reconstruct the cross-section has achieved an image correlation of 95.82%, and a mass error of 0.84%.

Figure 4 shows an ECHO model with values IC and ME, which correspond to image correlation and mean error, respectively. The original image, shown on the left, is passed through the same scanning and diagonalization method described previously. The capacitance matrix is similarly passed through the ECHO algorithm, which attempts to reconstruct the original cross-section based solely on the capacitance matrix. ECHO’s reconstructed image, displayed on the right, has IC and ME calculations attached to it, which is determined by overlaying the ground truth and reconstruction plots. In this example, the IC is 97.92% and the ME is 1.24%.

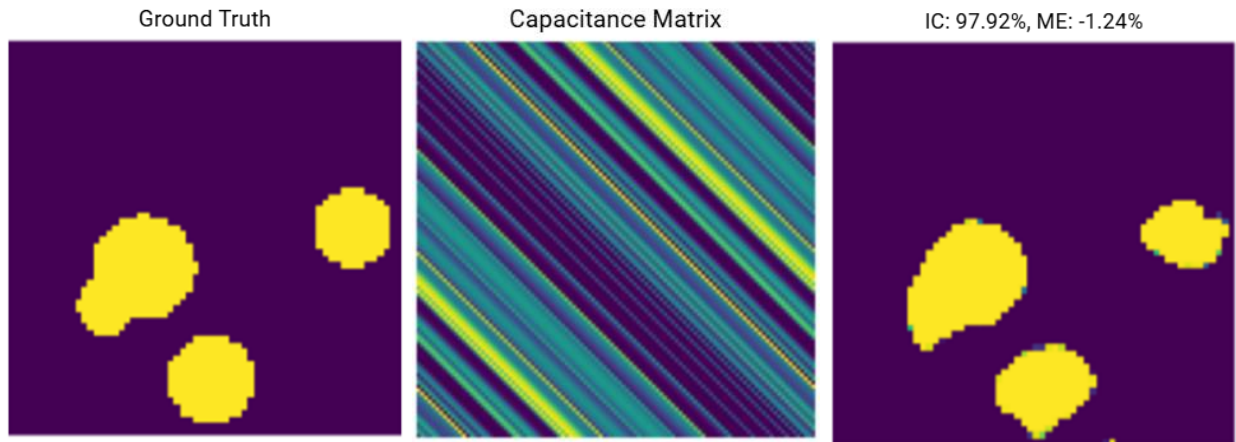


Figure 4: ECHO Four-Circle Demonstration

Currently, in a simulated environment with simplified training parameters, the ECHO algorithm, trained on 10,000 sample cross-sections over 3,500 epochs (training iterations), achieves an average of $94.4\% \pm 2.8\%$ image reconstruction correlation, $2.2\% \pm 1.1\%$ mass error, reconstruction speed of 20 ± 10 milliseconds, and an image resolution of 64×64 pixels. When tested on objects the model has not been trained on, like squares and circles of larger or smaller radii than in the initial training and testing sets, the model achieved an average of $90.1\% \pm 1\%$ image reconstruction correlation, and an average mass error of $6.8\% \pm 1.4\%$. These values were calculated at a 99% confidence threshold. It should be noted that the image correlation value is calculated by comparing every pixel in both the original and reconstructed images. Mass error is based only on the sum of the brightest pixels in the images. The reconstruction speed depends on the specifications of the computer running the algorithm. The measurements above were recorded from a CUDA[®] enabled NVIDIA[®] GeForce RTX™ 4060 Ti GPU. Additional benchmarks were performed on an 11th Gen Intel[®] Core™ i7-11800H at 50 ± 20 milliseconds. Finally, these values were calculated from simplified training data instead of simulations of the testing setup.

1.5.3. Analysis

Simulation of the ECHO sensor setup was carried out using ANSYS[®] Maxwell[®]. While initially a method for validating sensor data, Finite Element Analysis (FEA) has become a key component in gathering simulated measurements for training ML and improving the accuracy of the ECHO algorithm. Several

ANSYS® products were tested, and Maxwell® was chosen for its effective electrostatic solver that quickly computes capacitance. After carbon fiber nylon mix cross-sections are inserted into an air-filled sensor in Maxwell® (Figure 5), the capacitance between all unique electrode pairs can be gathered, the data is saved in a table, and the measurements are repeated with the cross-section in a new location.

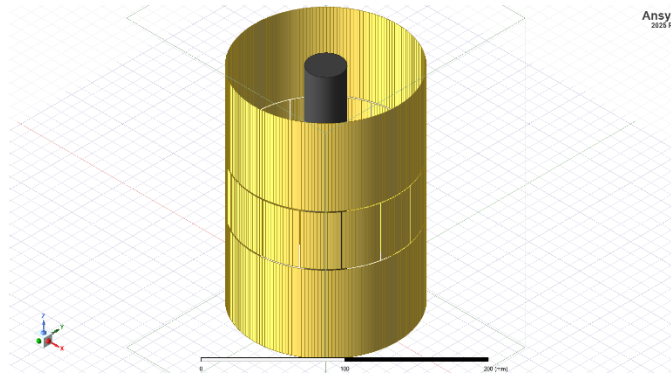


Figure 5: ANSYS Maxwell Simulation Setup

The simulated capacitance measurements are then processed by a MATLAB® code to be converted into impedance values and compiled into the training dataset. Each measurement scenario is labeled according to a naming scheme comprised of the position and size of the cross-section inserts, and then the algorithm can be used for data training.

1.6. Future Advancements

ECHO is currently in the early stages of Phase B in the NASA Systems Engineering Lifecycle and is developing the preliminary design for a full-scale model. To advance toward a fully functional system, several critical milestones must be met, the first being an improved design of the amplifying analog circuit as well as a minimally invasive sensor installation. In the meantime, resources for more realistic experiment conditions should be sought out. This includes, but is not limited to, physical tests under different pressure, temperature, density, area, permittivity, and number of electrodes. Together with high fidelity simulations, the ECHO algorithm will be trained under a much larger and more diverse dataset which ensures the system's performance under all conditions. Lastly, ECHO will iterate towards a domed sensor configuration. The three-dimensional system will be developed that can interpolate results from layered two-dimensional reconstructions into a full volumetric reconstruction of the propellant within the tank.

1.6.1. Electrode Integration

One primary objective of future iteration of the sensors is to mitigate any protrusions into the tank for wiring purposes. A solution may involve integrating ECHO directly into the walls of the tank. By manufacturing the tanks in such a way that the ECHO system is built into the walls of the tank, penetrative wiring could be avoided completely. In the event that integrating ECHO directly into the tank becomes infeasible, the use of a Flexible Printed Circuit Board (FPCB) and a single feedthrough for wire routing will remain a practical and low-risk solution. Additionally, electrode sizing plays a critical role in system performance. An ideal shape or size of electrode has yet to be determined, and future work will involve optimizing electrode dimensions to maximize system accuracy.

1.6.2. Domed Geometries

Future testing will involve demonstrating ECHO's capability to accurately gauge mass within domed geometries, and testing will be required to adapt the ML algorithm to this geometry. Specifically, the system utilizes a general algorithm that is tailored for individual tank designs. To adapt ECHO for a

curved geometry, ECHO will be trained with datasets including domed geometries by generating training data with known cross-sections and validating the algorithm's accuracy using physical tests.

1.6.3. Relevant Environment Testing

The current system is assessed to be between a TRL 3 and TRL 4, as the testing apparatus still requires minor improvements to validate core functionalities. One key consideration is the availability of training data representative of microgravity environments, which would place future iterations at a TRL 6. Currently, testing has been conducted under standard Earth gravity conditions. While these datasets provide a strong foundation for algorithm development, they may not fully capture fluid behavior, sloshing effects, and sensor response under reduced gravity. To address this, future work will explore physics-informed modeling and testing in simulated environments.

Further research will also focus on enhancing the ML algorithm's ability to account for sensor anomalies or failures. These improvements will be validated through targeted cryogenic testing to ensure system reliability under the desired operating conditions.

1.7. Verification

Through trade studies and short proposals, the potential effectiveness of several microgravity mass gauging techniques were compared. During the trade studies, emphasis was placed on feasibility, innovation, and current research (Table 4). ECHO was selected due to the relatively high accuracy of ECT, the relevant application of ECT technologies in tracking fluid flow, the ability to make measurements without acceleration, and the ability to innovate on current designs using ML.

1.8. Validation

Through analysis and preliminary testing, the team evaluated the efficacy of ECHO in an effort to promote the design of an accurate mass gauging system. Trade studies were conducted to determine what testing fluids (Table 5) and type of ML algorithm (Table 6) would be used. After further research, the team moved to begin training a basic version of the ML algorithm using an idealized data set and ANSYS® Maxwell® simulations to validate the testing data.

To validate ECHO's machine learning algorithm, a test apparatus was designed and built (Figure 6). The testing apparatus consists of a cryogenic dewar with an interior lined by a 15-electrode array on a polyimide FPCB. A custom lid was designed with a swappable mount for suspending various shapes of known cross-sections inside of the dewar. The lid is 3D-printed from polyamide carbon fiber filament to withstand cryogenic temperatures (Hohe et al., 2020). A connector on this FPCB protrudes out from the top of the dewar and is used to connect the electrodes to a CD4067 analog demultiplexer, which then completes the electrode connection to a DAQ through an opening in the lid. The DAQ used is a National Instruments USB-6421 with additional supporting circuitry to reduce stray capacitance. The DAQ interfaces with a Python script that processes the data and runs it through the ML algorithm.

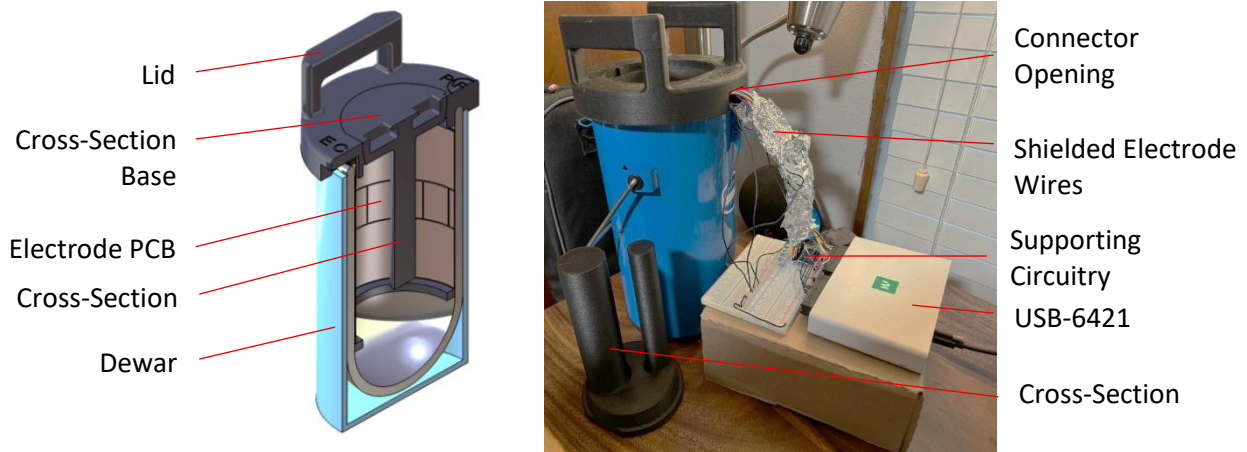


Figure 6: Test Apparatus Section View (Left) and Complete Setup (Right)

During initial testing, environmental and system noise prevented accurate results from being obtained with the testing apparatus. To mitigate these effects, a Butterworth bandpass filter and a Gaussian filter were implemented to reduce noise and clean up the received data. Hundreds of air tests were then conducted with the first three cross-sectional inserts (Figure 7).

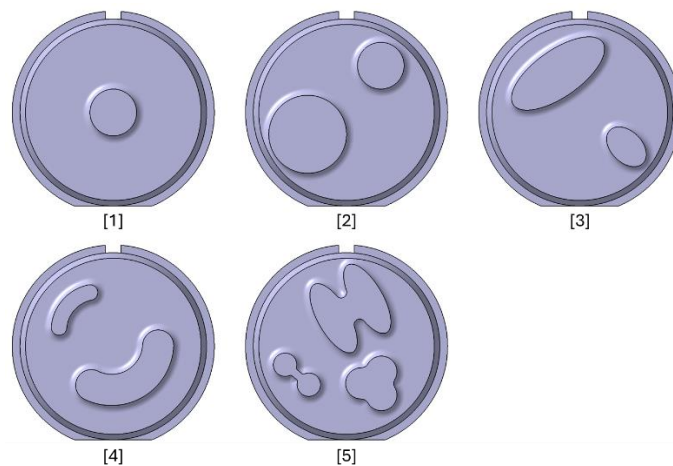


Figure 7: Cross-Section Inserts

During testing, it was noted that despite the cleaned data from the filters, the CGAN based ML algorithm inaccurately reconstructed the image based on the capacitance matrices (Figure 8). When the ML was fed an expected 105x105 dataset made up of idealized data to generate a circle in the middle of the “Generated Phantom” a diagonalized string of distorted shapes in the top right with a stray oblong line in the bottom left was generated. This demonstrated that refinement of both the algorithm and training dataset is necessary because the ML model likely drifted in training, making connections between the diagonal datasets of the capacitance matrix and diagonal/stretched shapes. With further refinement and improvements to data representation, by means of introducing noise into the training datasets to simulate real world conditions, the ML model’s robustness to environmental noise is expected to improve. These enhancements are anticipated to enable accurate and realizable image reconstruction during both testing and real-world implementation.

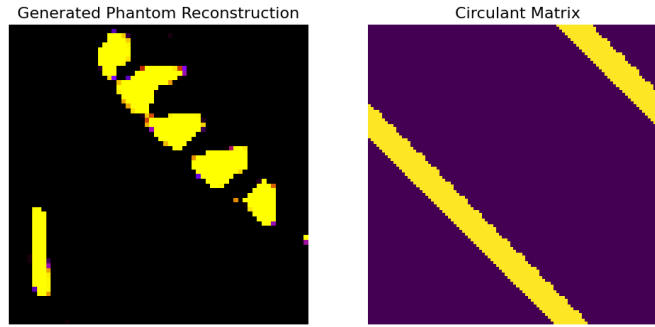


Figure 8: Idealized Circle Reconstruction

1.9. Risks

To analyze and mitigate any risks posed by the ECHO system, a risk management sheet and matrix were developed (Table 1). The risk sheet compiles 13 relevant risks to determine likelihood, consequences, and to evaluate mitigation plans. This analysis identified four critical risks, which relate to capacitor sensor failure, thermal insulation, acceleration inaccuracies, and communication interruptions.

Table 1: ECHO Risks Matrix

LIKELIHOOD	5			1		
	4		6	3, 4	2	
	3			5, 9		
	2	13	11	7		
	1			10	8, 12	
		1	2	3	4	5
		CONSEQUENCES				

Capacitor sensor failure (Risk 1) is when the electrodes return incorrect capacitance measurements, making the results inaccurate. To prevent this, mitigation plans could include increasing both electrode thermal insulation and reinforcing electrode connections to the tank walls. However, the likelihood of this occurring is unknown without proper testing results. The current plan is to watch for failure and modify the mitigation plan with more data.

Thermal insulation failure (Risk 2) could arise when the electrodes are directly exposed to cryogenic propellant in the tank. The current design incorporates an insulation cylindrical barrier between the electrodes and the tank wall; however, validation of this design will need to be conducted through experimental testing under cryogenic conditions. In addition to experimentation, further research including thermal modeling and simulation are needed to determine the reliability of the electrodes over extended time intervals.

Significant acceleration (Risk 3) can induce intense periods of propellant sloshing. Rapid sloshing poses a challenge to measurement accuracy if the propellant moves faster than ECHO's sampling rate, or if propellant resides in a region of the tank with poor accuracy. To address this, two solutions could be to

optimize ECHO’s measurement rate with experimental data, and to increase the number of electrodes in those regions. Future work for these solutions includes dynamic testing, such as vibration tests, to evaluate and enhance sensor performance under simulated launch and in-flight conditions.

Communication loss (Risk 4) between the ECHO system, the DAQ unit, or the spacecraft inhibits propellant measurements. To mitigate the risk of communication loss, one solution includes securing all data and power connections with robust harness design. To fully mitigate this risk, comprehensive simulations and testing the full integrated system will be required during later stages of development.

1.10. Full-Scale Implementation

While the current ECHO testing apparatus consists of a rudimentary ML algorithm and a single row of 15 electrodes, any full-scale implemented system will have to utilize tens or hundreds of rows, and an ML algorithm trained on larger and more diverse datasets. The increase in electrodes is necessary to facilitate an accurate three-dimensional reconstruction. On an HLS vehicle, such as SpaceX’s Starship, the size of the tank means that the maximum distance between two electrodes at a given cross section is 9 meters (SpaceX, 2025). The current ECHO setup, with a 6-inch diameter, has a sampling rate of 15,000 samples per second, an excitation frequency of 2kHz, and an applied electrode voltage of 1V. To combat increased distance, scaling up the ECHO architecture will require a notable increase in all these categories.

1.11. Budget

Utilizing the NASA Project Cost Estimating Capability (PCEC), an estimate for the costs associated with implementing ECHO on SpaceX’s Starship were obtained using a First-Pound Cost (FPC) Cost Estimating Relationship (CER). An FPC CER is an equation that generates a cost estimate based on system weight and is derived through regression analysis using the costs of similar existing systems. The CER used for this estimate is based on the costs of existing instrumentation subsystems on liquid stage launch vehicles. An input of 230 kg (507 lbm) was used, assuming the ECT system is implemented on Starship’s main liquid oxygen and methane tanks with aluminum electrodes that are 10 microns thick and a polyimide insulation layer that is 0.2 mm thick (Storey, 2023). Table 2 shows the cost output of the CER and their inflation-adjusted amounts.

Table 2: PCEC Cost Outputs (Millions of Dollars)

Cost Phase	FY2015 \$M	FY2026 \$M
Non-Recurring	29.2	36.5
Design & Development	23.5	29.4
System Test Hardware	5.7	7.1
Flight Unit (Recurring)	4.4	5.5
TOTAL	33.6	42.0

The non-recurring costs were inflation-adjusted and converted to an annuity distributed across the project life, assuming a 2.6% yearly interest rate. These costs were included along with a 50% manufacturing margin in the total direct costs of the project. Personnel salaries are also included in the overall cost estimate. Travel costs are neglected assuming personnel will be living in Huntsville, Alabama, and tests can be conducted at NASA’s Marshall Space Flight Center. Table 3 contains a breakdown of the current cost estimate for the project, excluding any changes that may occur to the cost of launching the mission.

Table 3: Full Budget Breakdown (Thousands of Dollars)

Mission Phase	Phase C	Phase C	Phase D	Phase D	
Year	FY 1 (2026)	FY2 (2027)	FY3 (2028)	FY4 (2029)	Total (\$K)
PERSONNEL					
Science Personnel	80	82	84	86	332
Engineering Personnel	320	328	337	345	1,330
Technicians	60	62	63	65	249
Administration Personnel	120	123	126	129	499
Project Management	240	246	252	259	997
Total Salaries	820	841	863	884	3,408
Total ERE	229	235	241	247	951
TOTAL PERSONNEL	1,049	1,076	1,103	1,131	4,359
DIRECT COSTS					
System Cost (from CER)	10,500	10,773	11,046	11,319	43,638
Manufacturing Margin (50%)	5,250	5,387	5,523	5,660	21,819
Total Direct Costs	15,750	16,160	16,569	16,979	65,457
FINAL COST CALCULATIONS					
Total Projected Cost	16,799	17,236	17,672	18,109	69,816
Total Cost Margin (30%)	5,040	5,171	5,302	5,433	20,945
Total Project Cost	21,839	22,406	22,974	23,542	90,761

1.12. Project Timeline

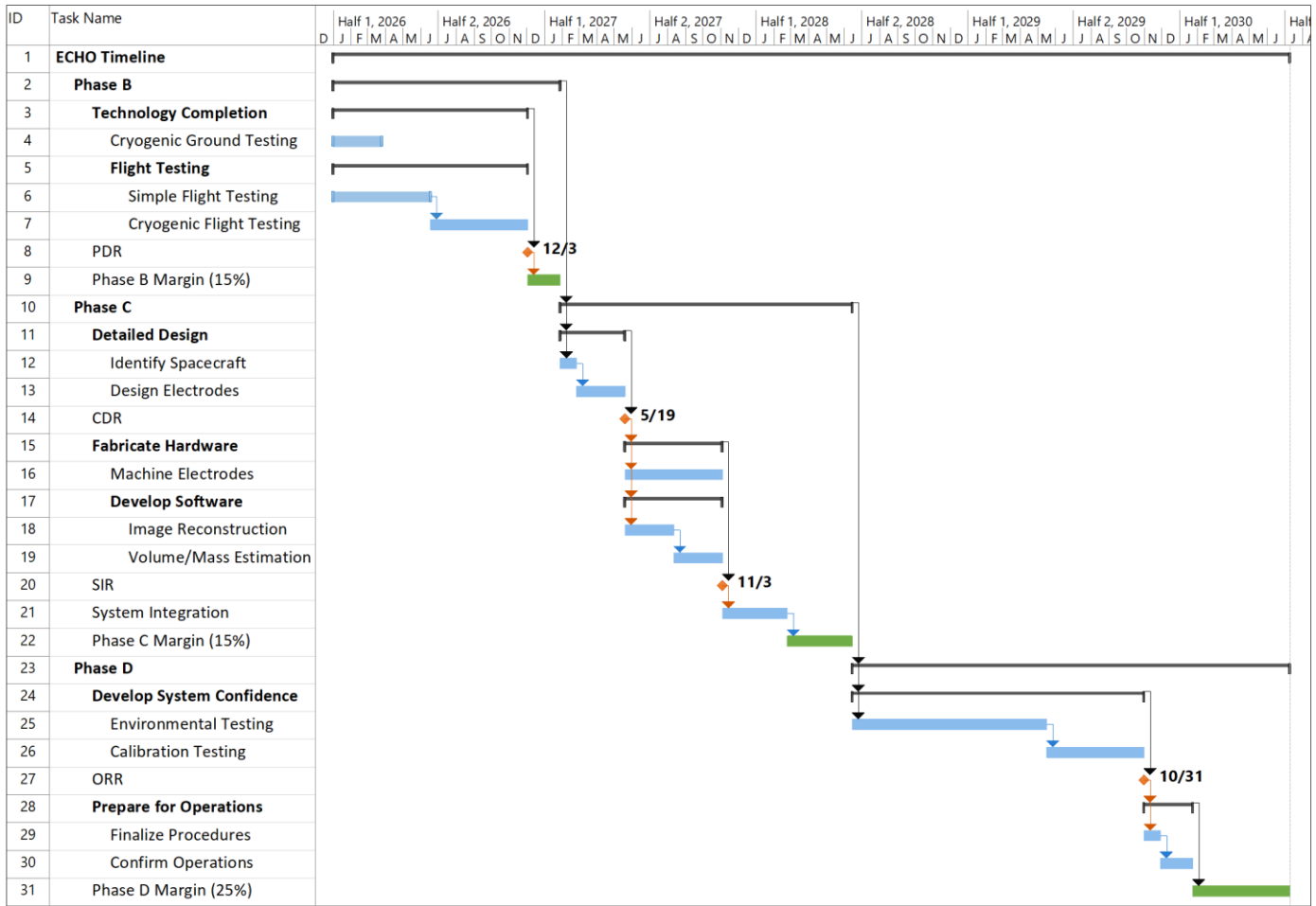


Figure 9: ECHO Development Timeline

The phases of ECHO’s development have been laid out into a five-year timeline (Figure 9) with a twelve-month margin. Major milestones were based on the NASA Systems Engineering Handbook (Hirshorn, 2007). The blue bars represent major tasks, the orange diamonds represent major checkpoints, and the green bars represent the margin for each phase of the development.

Phase B focuses on the continued preliminary design and further technology, including small-scale flight testing and cryogenic tests. With ECHO’s current testing configuration, it is likely that cryogenic ground tests could be conducted in roughly three to four months. The testing configuration can also be modified for a simple flight test to gather real-time data in a changing environment. These flight tests would ideally be conducted with a drop tower or onboard an aircraft with a parabolic trajectory. Phase B will then end with a Preliminary Design Review and achieve a TRL of 6.

Phase C focuses on final design and fabrication of the system for the chosen spacecraft. Once the spacecraft is determined, the electrodes can be designed around the specified propellant tank. Following the Critical Design Review, electrode manufacturing can begin, and the ECHO algorithm can be trained using simulated data. Once the electrodes have been produced and the algorithm has been trained, a System Integration Review can be conducted, and ECHO can be integrated with the rest of the spacecraft.

Phase D focuses on the system assembly, integration, and testing in preparation for full-scale flight testing and operations. System confidence will be ensured through continued testing and calibration of the ECHO algorithm for the designated tank. Phase D will also include environmental and vibrations testing to ensure a successful integration. Then the Operational Readiness Review will be conducted to approve ECHO for use on space missions, achieving a TRL of 7.

1.13. Conclusion

The team has spent the past year developing ECHO through intensive research, trade studies, and testing, resulting in a working prototype featuring a 1x15 electrode array with an ML image reconstruction algorithm. The system operates by measuring capacitance between distinct electrode pairs by sending and receiving AC voltages through a DAQ-Demultiplexer-Electrode circuit. These measurements are recorded into a 1x105 array which the ECHO algorithm converts into a capacitance matrix to reconstruct a cross section of the tank contents. Testing has demonstrated that ECHO is a promising solution to mass gauging in microgravity environments through a series of ground-based experiments and simulations. In the future, the team plans to continue development of ECHO beyond the HuLC forum. Next steps include developing a new ML model, trained on realistic data sets, and adding more rows of electrodes to the testing setup to support three dimensional measurements.

References

- Deabes, W., & Abdel-Hakim, A. E. (2024). CGAN-ECT: Reconstruction of electrical capacitance tomography images from capacitance measurements using conditional generative adversarial networks. *Flow Measurement and Instrumentation*, 96. <https://doi.org/10.1016/j.flowmeasinst.2024.102566>
- Hirshorn, S. R. (2007). *National aeronautics and space administration*
- Hohe, J., Neubrand, A., & Fliegenger, S. (2020). *Performance of fiber reinforced materials under cryogenic conditions* <https://doi.org/10.1016/j.compositesa.2020.106226>
- Lee, D., Cho, M., Choi, H., & Tahk, M. (2018). A study on the micro gravity sloshing modeling of propellant quantity variation. *Transportation Research Procedia*, 29, 213. <https://doi.org/10.1016/j.trpro.2018.02.019>
- Mirza, M., & Osindero, S. (2014). *Conditional generative adversarial nets*
- SpaceX. (2025). *SpaceX starship*. www.spacex.com. <https://www.spacex.com/vehicles/starship/>
- Storey, J. M., Marsell, B., Elmore Mike, & Clark Scott. (2023). *Propellant mass gauging in microgravity with electrical capacitance tomography*.
- Sun, S., Lu, X., Xu, L., Cao, Z., Sun, J., & Yang, W. (2021). Real-time 3-D imaging and velocity measurement of two-phase flow using a twin-plane ECT sensor. *IEEE Transactions on Instrumentation and Measurement*, 70, 1. <https://doi.org/10.1109/tim.2021.3073934>
- Wanta, D., Smolik, A., Smolik, W. T., Midura, M., & Wróblewski, P. (2024). Image reconstruction using machine-learned pseudoinverse in electrical capacitance tomography. *Engineering Applications of Artificial Intelligence*, 142. <https://doi.org/10.1016/j.engappai.2024.109888>

York, T. (2001). Status of electrical tomography in industrial applications. <https://doi.org/10.1117/1.1377308>

Zheng, J., Li, J., Li, Y., & Peng, L. (2018). A benchmark dataset and deep learning-based image reconstruction for electrical capacitance tomography. *Sensors*, 18(11) <https://doi.org/10.3390/s18113701>

Zimmerli, G. A. (2007). Propellant gauging for exploration.

Doherty, M. P., Gaby, J. D., Salerno, L. J., & Sutherlin, S. G. (2010). *Cryogenic Fluid Management Technology for Moon and Mars Missions*. <http://www.sti.nasa.gov>

Storey, J. M., Elmore, M. T., Solutions, I., & Clark, S. (2023). *Propellant Mass Gauging in Microgravity with Electrical Capacitance Tomography*. <http://www.sti.nasa.gov>

Yendler, B., Chernikov, S., Molinsky, J., & Guadagnoli, D. (2014). Comparison of gauging methods for orbital's GEOstarTM1 satellites. *13th International Conference on Space Operations, SpaceOps 2014*. <https://doi.org/10.2514/6.2014-1810>

Appendix

Table 4: Microgravity Mass-Gauging Methods Trade Study

Criteria	Weight	Scale	Dorthy System	X-Ray Tomography	Radio Frequency Mass Gauging	Modal Gauging	Electrical Capacitance Tomography	Thermal Tomography	Bladder
Testability	15%	3-0.	0	1.5	3	3	3	3	3
Difficulty (In our favor)	15%	3-0.	0	2	2.5	2.5	2	3	1
Interest/Preference	10%	3-0.	3	2	3	2	3	2	2.5
Innovation	20%	3-0.	3	2.5	2.5	2.5	2.5	1.5	3
Past Knowledge	5%	3-0.	0	1	2	1	1	1.5	1
Feasibility of Implementation	20%	3-0.	0	1.5	1.5	2.5	2.5	2	1
Available Information	15%	3-0.	1	2.5	2.5	3	3	3	1
Weighted Total %	100%		35%	65%	80%	84%	85%	78%	62%

Table 5: Testing Fluids Trade Study

Criteria	Weight	Scale	Liquid Nitrogen	Vegetable Oil	LN2 + Oil	LN2 + Air	Air	Water
Time Commitment	30%	3-0.	2	2.5	1	1.5	3	2
Accuracy	30%	3-0.	3	2	3	3	2	1
Hazard Level	25%	3-0.	1.5	3	1.5	1.5	3	3
Interest	15%	3-0.	3	2	2.5	3	1.5	1
Weighted Total %	100%		78%	80%	65%	73%	83%	60%

Table 6: Machine Learning Algorithms Trade Study

ML Trade Study		Scores		Trades									
Criteria	Weight	Scale	GCNN	CGAN*	ADMM*	FFNN	SVM	U-Net	Hopfield Networks	SegNet*	CN	Autoencoder	L-ELM
Existing Research	10%	1-3	3	3	2	1.5	2.5	3	2.5	3	1.5	3	1.5
Relevance/Implementability	10%	1-3	3	2.5	2.5	1.5	2.5	2.5	2	3	2	2	2.5
Accuracy/Performance	20%	1-3	2	3	2.5	1	1.5	2	1	2	1.5	1.5	1.5
Timeframe	25%	1-3	3	2	2	1	2.5	1.5	1	3	3	1	2.5
Difficulty (In our favor)	15%	1-3	2	2	2.5	1	2.5	2	1	2	2.5	1	2
Interest/ Preference	5%	1-3	3	3	2	2	2.5	3	1	3	1	2	1.5
Innovation	15%	1-3	1.5	2.5	2.5	3	2	2.5	3	1.5	1.5	1.5	2.5
Weighted Total %	100%		81%	83%	77%	48%	74%	72%	52%	81%	68%	51%	69%

Table 7: ECHO Risks Matrix

ID	Risk Name	Description	Related Systems	L	C	Method	Plan
1	Capacitor Sensor Error	Capacitors sensors transmits incorrect data leading to potentially inaccurate mass gauging data.	Electrodes	5	3	W	Accurate calibration corrects this issue
2	Thermal Insulation Failure	If the parts of ECHO that are not designed to come in contact with the tank walls do come in contact with the cryogenic tank walls, or if the insulation for the intended parts fail, it may cause damage to the system.	Tank Insulation	4	4	R	Research different materials to use as insulation around tank prevents systems from touching the tank.
3	Inaccuracy due to Acceleration	In periods of acceleration, the fluid-mass, if small enough, may concentrate in a region without enough sensors to gather data. This may cause errors in the reconstruction of data or even provide false readings.	ECHO, Propulsion , HLS	4	3	M	Place additional arrays of sensors in issue-prone areas i.e. the ends of the tank.
4	Communication Interruption	During communication from the sensors, to the DAQ to the computer, any breakdown of communication could lead to no or incorrect data being transferred.	DAQ	4	3	M	Ensure connections are secured before and after test procedure.
5	ECHO Mass	To accurately measure the mass of the full HLS propellant tanks, the mass of the ECHO system may exceed the critical point of mass where the inconvenience associated with mass exceed the convenience of having the measurement system.	ECHO, Propulsion , HLS	3	3	M	Reduce ECHO system mass and size without reducing the system's accuracy.
6	ECHO Volume	The amount of volume the ECHO system takes up in the propellant tank will reduce the amount of propellant HLS could carry, reducing mission efficiency.	ECHO, Propulsion , GNC	4	2	A	The volume of the ECHO system could be reduced for efficiency, but few mitigation options are available.

7	Power Consumption	The power it takes to run the ECHO system on the Starship scale exceeds the allotted power for the ECHO system by the HLS EPS	EPS, ECHO	2	3	W	ECHO would be designed with a set power budget, comparisons would be needed to determine if the electrical requirement would that given by HLS.
8	Computer Memory/Processing Failure	Computer is unable to process information or handle new tasks until memory is freed. This would lead to incomplete data sets and incomplete mass gauging information.	ECHO, Power	1	4	W	Ensure hard disks have enough space to record all data with extra space for redundancy.
9	Radiation Environment Affecting Data	Computing and DAQ system are exposed to radiation environment leaving the potential for corruption of data by interacting with charges in memory systems.	ECHO, Starship	3	3	R	Research the average radiation environment in cislunar space and different shielding materials
10	Premature Test Failure	During testing, if ECHO's function ends prematurely, i.e.. before the end of the test period, it would lead to incomplete data sets and thus potentially incomplete mass gauging information.	ECHO, Power	1	3	W	Recalibrate testing apparatus, ensure all components are functioning, and re-run the test
11	Immobilization By Orientation	In case of the issue of sensors slightly coming detached or even completely detached, it may impact the quality of measurements.	Electrodes	2	2	W	Observe during testing and adjust if issue becomes prevalent. If it does, adjust adhesives or placement to ensure sensors do not become dislodged.
12	Computing System Protection Failure	If the ECHO system's DAQ or computer is not properly protected to potential violent forces, it could cause a failure of the system overall.	ECHO, DAQ	1	4	A	Ensure all parts are away from any hazards and maintain a careful posture when moving apparatus.
13	Software Module Data Error	Error with data from different modules, whether that be an error passing, casting, or modifying data.	DAQ	2	1	M	Calibrate and test program before full testing to ensure little/no error.

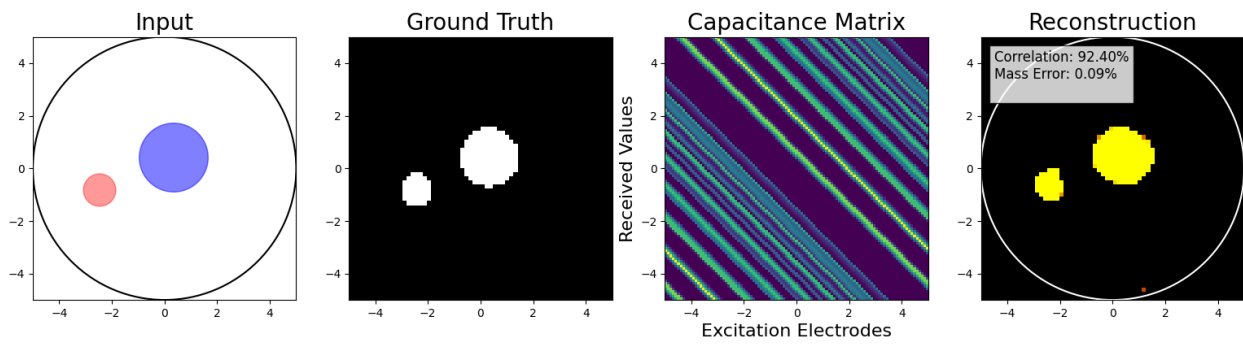


Figure 10: Extra Test 1

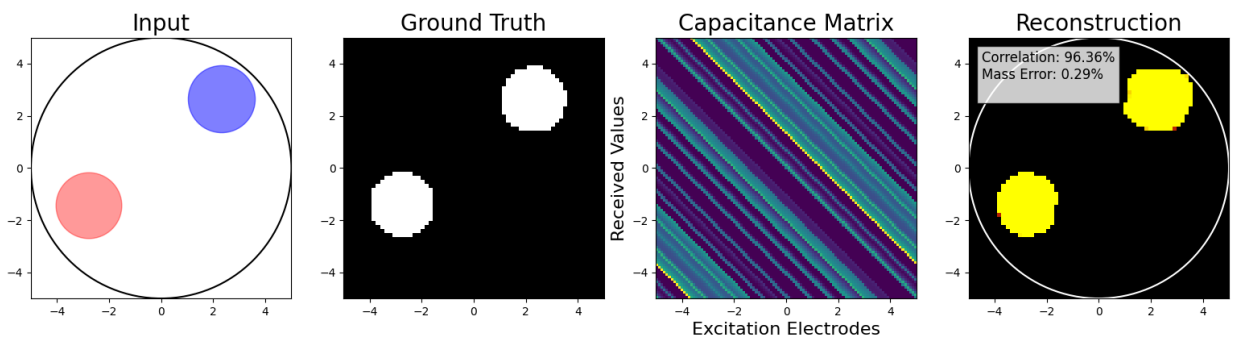


Figure 11: Extra Test 2

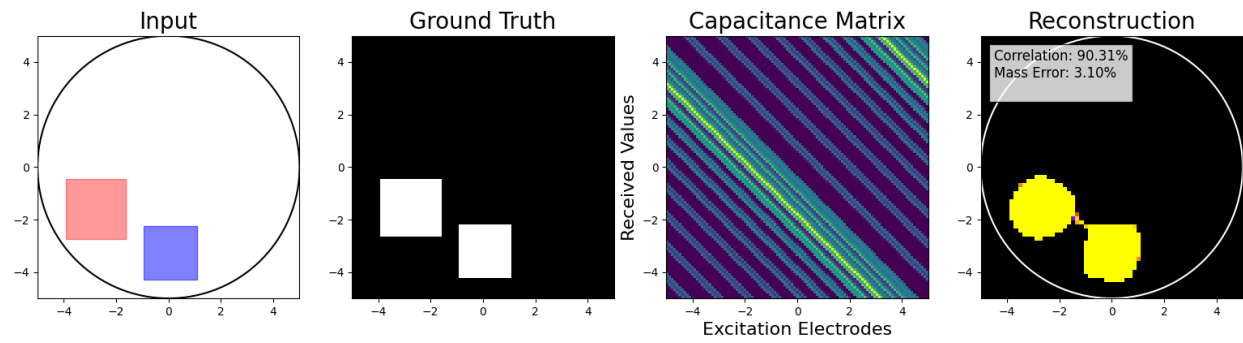


Figure 12: Extra Test 3

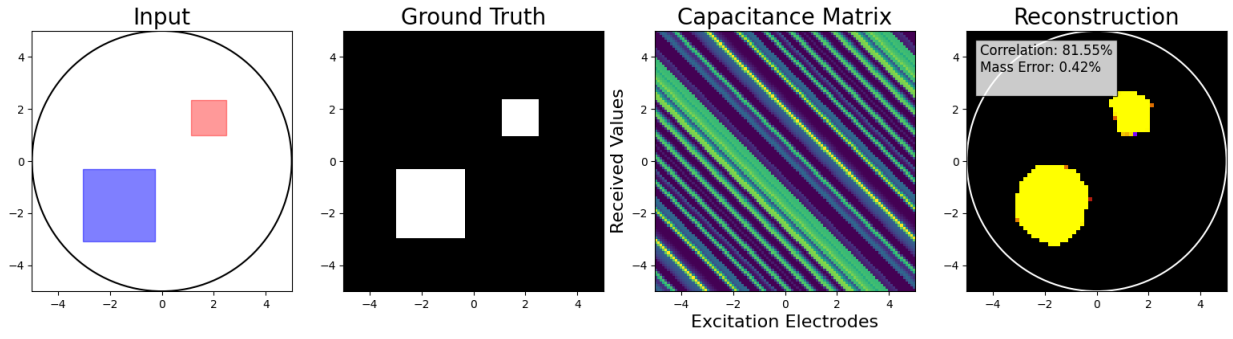


Figure 13: Extra Test 4

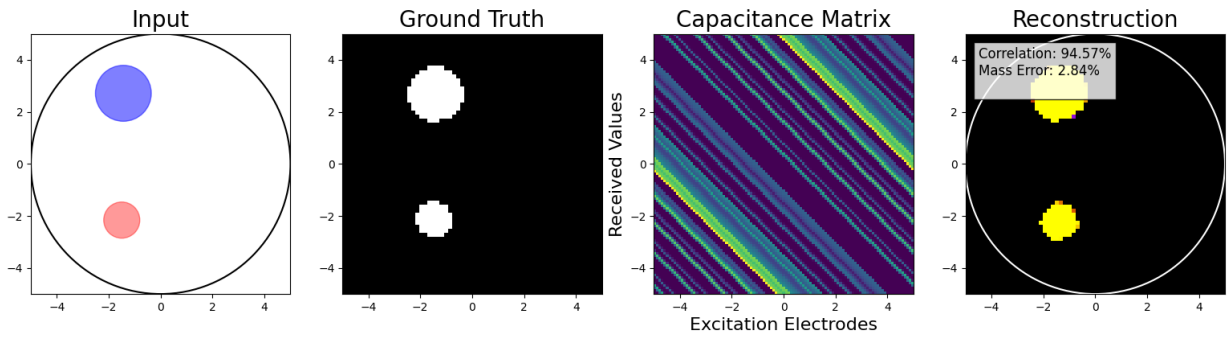


Figure 14: Extra Test 5

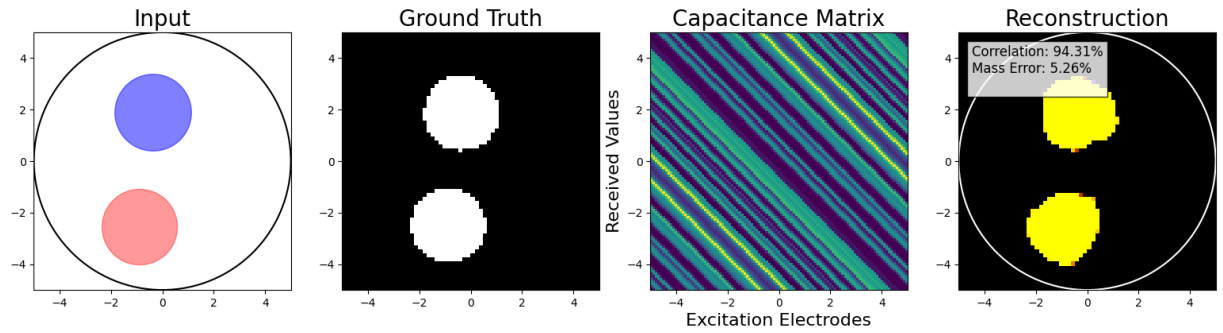


Figure 15: Extra Test 6

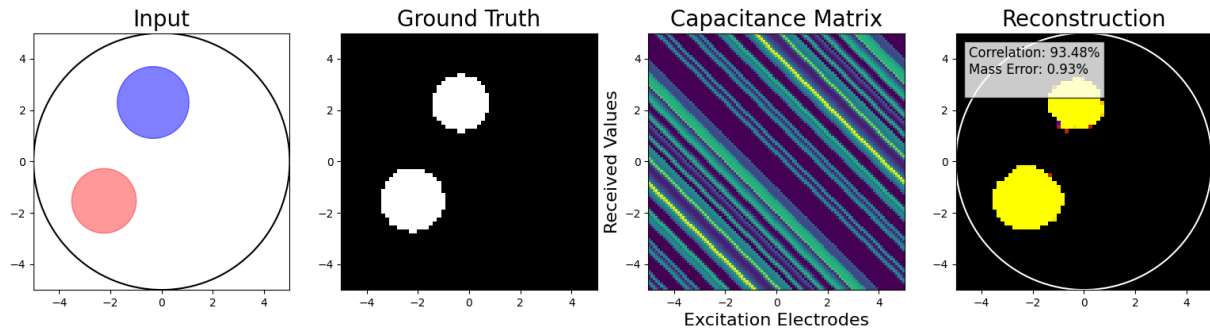


Figure 16: Extra Test 7

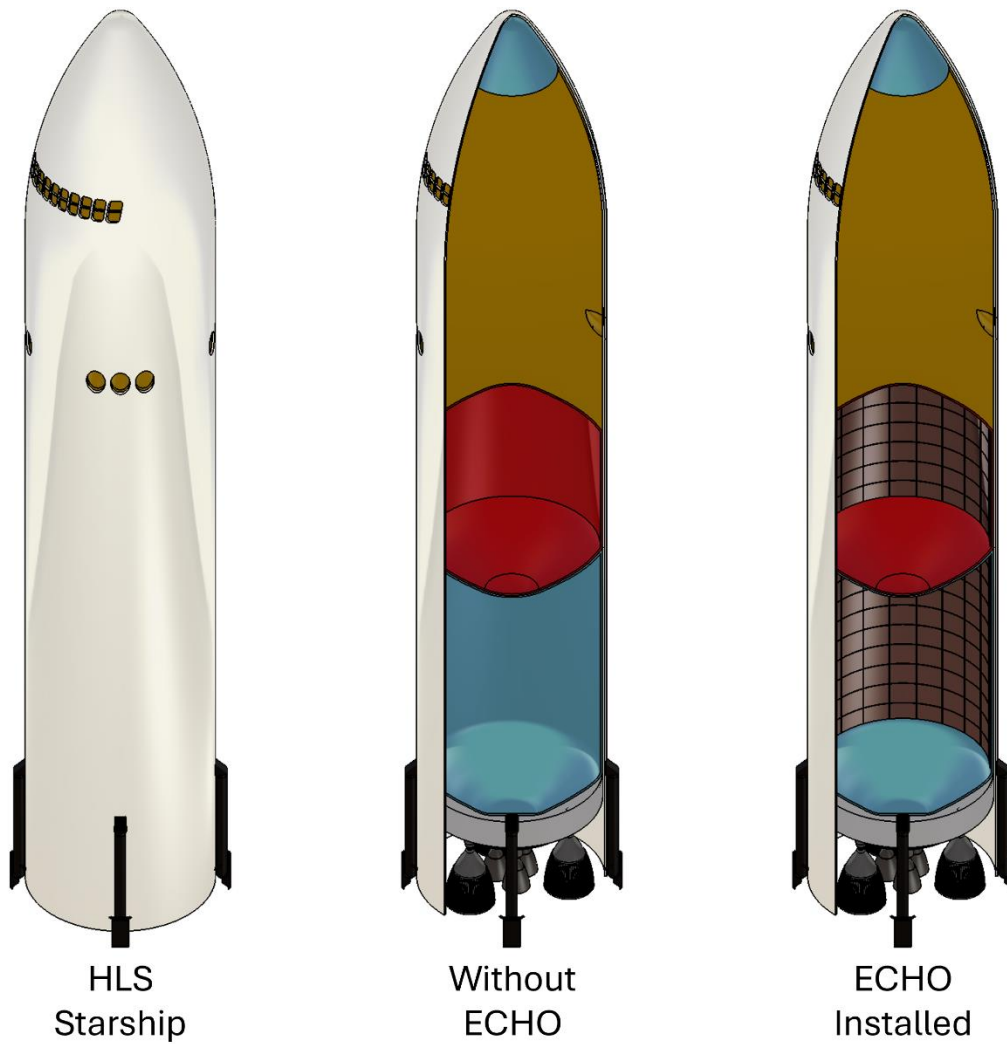


Figure 17: HLS Starship Progression